Thermochimica Acta, 64 (1983) 15–26
Elsevier Science Publishers B.V., Amsterdam – Printed in The Netherlands

KINETICS AND MECHANISM OF THE DEHYDRATION OF HYDRARGILLITES. PART II

R. NAUMANN, K. KÖHNKE

Chemistry Section, Mining Academy Freiberg, 9200 Freiberg (G.D.R.)

J. PAULIK and F. PAULIK

Institute for General and Analytical Chemistry, Technical University of Budapest, Budapest (Hungary)

(Received 19 August 1982)

ABSTRACT

When studying the thermal decomposition of various hydrargillites in Part I of this work, we found two borderline cases in the decomposition behaviour for artificial and natural hydrargillite. These two cases are especially characterized by the fact that no boehmite formation occurred with special natural hydrargillite compared to the artificial material. The thermal decomposition was studied to clarify the causes of these results taking into account the sample parameters, such as grain size, lattice defects, primary particle size and impurity content. The results show that the decomposition of hydrargillite is determined by the degree of defects in the crystal lattice and the primary particle sizes. The formation of boehmite from hydrargillite is complicated by the increase of the lattice defects with a simultaneous decrease of the primary particle size. This effect is independent of the grain size, the nature and the content of inserted alkali ions ($0.04\% \leqslant C_{Na,K,Rb} \leqslant 0.25\%$). The effect of the lattice defects on the mechanism of the thermal decomposition is discussed on the basis of the hydrargillite structure.

The statement obtained from quasi-isothermal measurements that the decomposition of hydrargillite into boehmite is a nucleation-controlled step, is supported by optical investigations. The smallest electron-optically observed nuclei are in the order of magnitude of the primary particles of the hydrargillite.

INTRODUCTION

In the first part [1] of this contribution we reported on our observations regarding the decomposition mechanism of hydrargillites by means of quasi-isothermal–quasi-isobaric thermogravimetry [2,3] and X-ray examinations and drew several conclusions. Among others, we showed that the decomposition of artificial hydrargillites consists of three partial reactions

$$\alpha\text{-Al(OH)}_3 \rightarrow \alpha\text{-AlOOH} + \text{H}_2\text{O} \quad (1)$$

$$2\ \alpha\text{-Al(OH)}_3 \rightleftarrows \chi\text{-Al}_2\text{O}_3 + 3\ \text{H}_2\text{O} \quad (2)$$

0040-6031/83/$03.00

$$2\ \alpha\text{-AlOOH} \rightleftarrows \gamma\text{-}Al_2O_3 + H_2O \qquad (3)$$

Each of these partial reactions is divided into further partial processes, some of which take place in a quasi-isothermal, some in a non-isothermal way, and one part of them leads to equilibrium whereas the other part does not. We also showed that the decomposition of natural hydrargillites only takes place in the borderline case according to eqn. (2) and no boehmite is formed. However, between the two borderline cases the transition regarding the decomposition mechanism is continuous.

Within the scope of this work we intend to discuss the question of which properties of hydrargillite have a considerable effect on the phase formation in the thermal decomposition. In this connection some aspects such as grain size, lattice defects and foreign-ion content of the hydrargillite are investigated. The results and possible conclusions are summarized in the present work.

EXPERIMENTAL

Samples and their pretreatment

One of our samples, hydrargillite I, was prepared in the laboratory by dilution of sodium aluminate. The thermoanalytical properties (curves 1 and 5, Fig. 1 and curve 1, Fig. 2) and the X-ray data are identical with artificial hydrargillite VI in part I of this work [1]. The chemical analysis of the foreign ions has shown 0.060% SiO_2, 0.019% Fe_2O_3 and 0.354% Na_2O. This product was used because its grain size corresponds to that of natural hydrargillite.

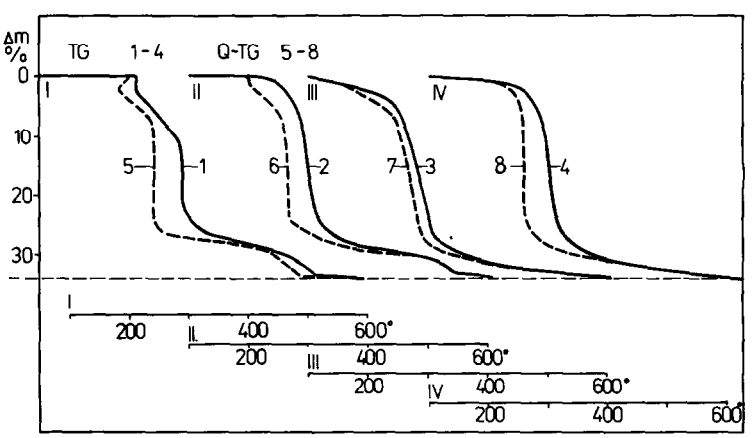

Fig. 1. TG curves (1–4) and Q-TG curves (5–8) of the decomposition of the different hydrargillites (I, II, III and IV) in open (1–4) and labyrinth crucibles (5–8).

The hydrargillite was ground in a disc vibration mill. Samples prepared with an agate disc and with a grinding time of 1 hour are numbered II and those being prepared with a steel disc and a grinding time of 10 min are

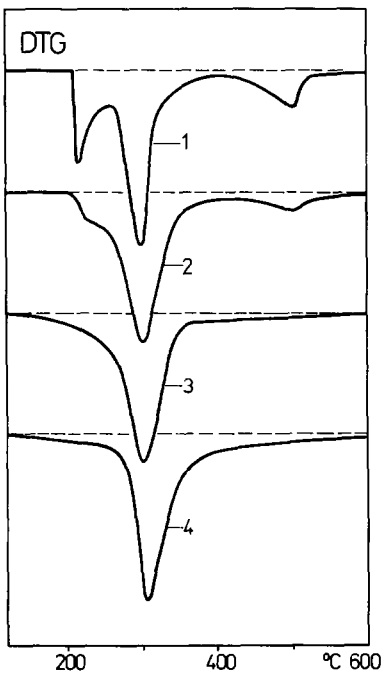

Fig. 2. DTG curves of the decomposition of the different hydrargillites (I, II, III and IV) in open crucibles.

numbered III. The thermoanalytical results are shown in curves 2, 3, 6 and 7 of Fig. 1 and curves 2 and 3 of Fig. 2. For comparison, the TG and DTG curves of a natural hydrargillite of Hungarian (Szőc) origin, numbered IV, are also illustrated in Figs. 1 and 2. X-Ray examination has shown the following interferences and intensities (values in parentheses): 4.83 (100); 4.36 (30); 4.23 (15); 2.38 (10); 2.45 (9). This sample is identical with our sample numbered I in Part I of this work [1].

Using a sedigraph 5000, made by Micromeritics, U.S.A., the particle size distribution for each sample was determined. For this purpose the samples are immersed in a solution of 0.05% Na_3PO_4 in distilled water and then ultrasonically treated until constant particle-size distribution was obtained. The results are given in Fig. 3.

In order to examine the influence of foreign ions on the thermoanalytical properties we precipitated hydrargillites with different degrees of purity from the sodium, potassium and rubidium aluminate solutions by dilution. The percentage of Na_2O, K_2O and Rb_2O of these samples was between 0.04 and 0.25%.

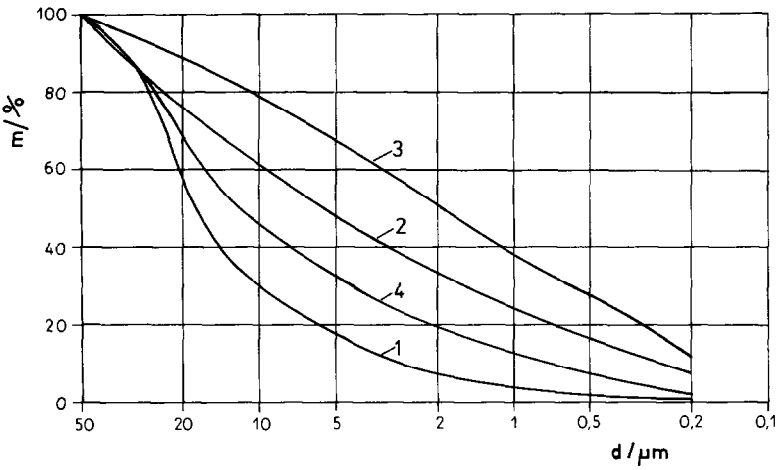

Fig. 3. Particle size distribution of the different hydrargillites (I, II, III and IV). m = Cumulative mass percent, d = equivalent spherical diameter.

X-Ray investigations

For the X-ray investigations the same apparatus as described in Part I of this work [1] was used. Determination of the lattice defects of the hydrargillites was carried out on the basis of the method according to Fricke and Gwinner [4]. For analysis the interference combinations 210/311, 210/222, 210/322, 311/222 and 222/322 of the single samples were used. Furthermore, according to a second method the single interferences were related to those of the undisturbed hydrargillite (sample I). Consistent results were obtained with both methods. According to Kochendörfer [5] the primary particle sizes were obtained from the half maximum intensities of the single interferences. The results of the investigated samples are summarized in Table 1.

TABLE 1

Primary particle size and lattice defects of different hydrargillites

Hydrargillite sample	Primary particle size (μm)	Lattice defects (nm)
I (artificial)	0.055	
II (artificial—ground with agate)	0.048	0.015
IV (natural)	0.036	0.028
III (artificial— ground with metal)	0.029	0.032

Thermoanalytical examinations

The conventional [2], as well as quasi-isothermal–quasi-isobaric thermogravimetric examinations [2,3], were performed by means of a derivatograph Q (Hungarian Optical Works, MOM, Budapest). Curves 1–4 of Figs. 1 and 2 were plotted for hydrargillites I–IV with a dynamic heating rate of 5°C min^{-1} in an open crucible in the presence of air. The weight of the samples amounted to about 300 mg.

For comparison, the conventional TG curves (curves 1–4) and the Q-TG curves (curves 5–8) of the same samples are shown in Fig. 1. These latter were obtained by applying the quasi-isothermal–quasi-isobaric measuring technique [2,3]. The sample with a weight of 300 mg was placed in an open crucible and heated in the weight-constant period at a heating rate of 3°C min^{-1}. The dehydration process was controlled with a decomposition rate of 0.3 mg min^{-1}, calculated for 100 mg total weight change.

Optical investigations of thermally pretreated hydrargillites

The question arose as to what way the boehmite phase, formed in the first period of the decomposition [1] of artificial hydrargillites, would influence the crystal surface. For the purpose of examination by means of a phase-contrast microscope and a scanning electron microscope, sample I was heated in a labyrinth crucible under quasi-isothermal–quasi-isobaric conditions (0.3 mg min^{-1} decomposition rate) up to the point where the sample lost 4% of its weight (curve 1, Fig. 1). With the weight loss of 4% heating was interrupted and the reaction was quenched by sudden cooling. For the phase-contrast investigations a Peraval Interphako microscope (VEB, Carl Zeiss, Jena) was used. Single crystals of the sample were immersed in a mixture of cinnamon aldehyde and oxalic acid diethyl ester (refraction index $n = 1.570$). The observations were made by application of the negative phase contrast with an enlargement of 1 : 1000. The scanning electron photographs were taken using the equipment of the Japanese company Jeol.

DISCUSSION

Thermodynamic consideration

Prior to a discussion of the various basic factors which were the subject of our investigations concerning the process of the thermal decomposition of hydrargillite into boehmite [eqn. (1)] or aluminium oxide [eqn. (2)], the position of the equilibria of these reactions is first considered.

In Fig. 4 the temperature dependence of the equilibrium constants K of these reactions is compared with the Q-TG curve of the artificial hydrargil-

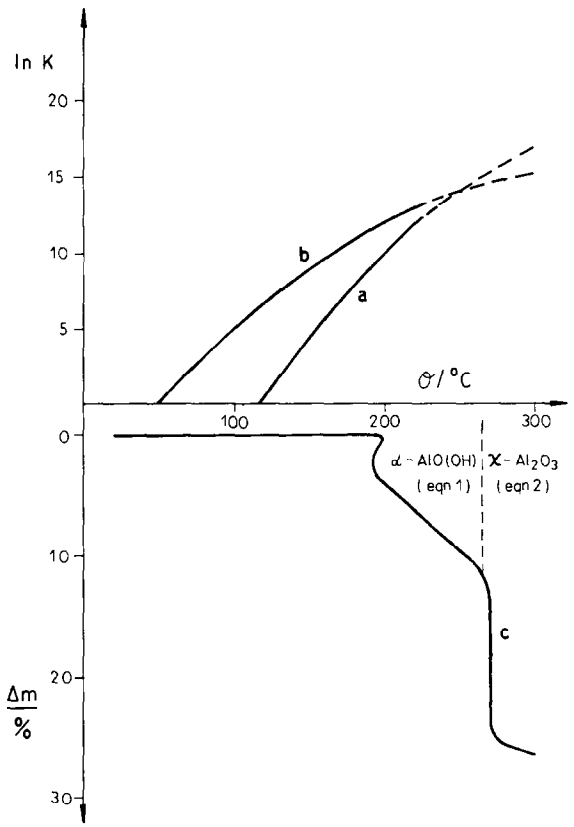

Fig. 4. Comparison of the calculated temperature dependences of the equilibrium constants (K) of the decomposition of hydrargillite into aluminium oxide according to eqn. (2) (curve a) and into boehmite according to eqn. (1) (curve b) with the experimentally obtained decomposition (Δm = weight loss) of hydrargillite under quasi-isothermal conditions in a labyrinth crucible (curve c).

lite (sample I). The equilibrium constants were caculated from the thermodynamic data of the reactants by means of the data given in the literature [6], and in the case of aluminium oxide in eqn. (2) the values of α-Al_2O_3 were used by approximation.

From the dependence of the equilibrium constants on the temperature it follows that under standard conditions the formation of boehmite (curve b, Fig. 4) above 49°C and of aluminium oxide (curve a, Fig. 4) above 117°C is possible. In the temperature range up to the intersection point of both curves at 247°C the decomposition equilibrium of the hydrargillite further lies on the side of boehmite and then inversely on the side of aluminium oxide. The results of quasi-isothermal thermogravimetric and X-ray experiments are in accordance with these calculations. As shown in Part I of this work [1], the decomposition of artificial hydrargillite begins at 200°C (curve c, Fig. 4), the

boehmite formation ends at 265°C (reaction 1) and thereafter only aluminium oxide is formed (reaction 2).

With natural hydrargillite (sample IV) no formation of boehmite can be detected by X-ray photography (curves 4 and 8, Fig. 1, curve 4, Fig. 2). The position of the decomposition temperature corresponds to the aluminium oxide formation of the artificial hydrargillite (curve c, Fig. 4).

A comparison of the equilibrium constants of the reaction equilibria according to eqn. (1) and (2) with the experimentally obtained phase components of boehmite and aluminium oxide shows that the kinetics of the reactions are highly inhibited. However, the obtained phase components are qualitatively reproduced by the differences of the equilibrium constants. Thus, the aleady discussed different inhibitions of the boehmite formation reaction of the investigated hydrargillite samples cannot be defined thermodynamically.

Investigation of the grain size effect

To investigate the influence of the grain size on the decomposition behaviour, sample I was graded into size fractions. However, this method did not yield any expressive results as the samples, due to classification, are mechanically stressed, and thus no definite grain size effect can be observed. For example, after remixing of the size fractions we found a modified decomposition process of the artificial hydrargillite which is identical to that of sample II which was ground in a vibrating mill (curves 6 and 2, Fig. 1; curve 2, Fig. 2). Therefore, an investigation of the grain size effect on recrushed or classified samples is not advisable.

The artificial hydrargillite (sample I) prepared by us has a grain size distribution similar to that of natural hydrargillate (sample IV) (curves 1 and 4, Fig. 3). By way of contrast, these samples represent the borderline cases in the thermoanalytical behaviour (curves 1, 4, 5 and 8, Fig. 1; curves 1 and 4, Fig. 2). The small excess of fines of the sample IV compared with sample I cannot explain the differences in thermoanalytical behaviour, because sample II contains even more fines (curve 2, Fig. 3) but its decomposition behaviour closely corresponds to that of artificial hydrargillite (curves 6 and 2, Fig. 1; curve 2, Fig. 2). The results show that the grain size of the hydrargillite is not definitely related to the decomposition behaviour.

Effect of lattice defects and primary particle size

By controlled grinding of the artificial hydrargillite (sample I) lattice defects in the hydrargillite were produced. The primary particle size of the crystallites is reduced by insertion of lattice defects. The results are summarized in Table 1. Increased lattice defects result in a decrease in the

primary particle size of the hydrargillite. The order of magnitude of the lattice defects and the size of the primary particles in the case of natural hydrargillite (sample IV) are in the range of the mechanically treated artificial hydrargillite (sample III). Obviously, deviations of the lattice structural elements from the normal positions in the lattice are obtained under the conditions of formation in nature.

The presence of lattice defects in samples II, III and IV can also be shown in the IR spectra. In accordance with the data of Korneva et al. [7] and Lukjanova et al. [8] who compared the IR spectra of various ground artificial hydrargillites, we found an intensity drop of the absorption bands of the OH-groups compared with the undisturbed sample I in the range 500–600 cm^{-1}, 975 cm^{-1} and 3400 cm^{-1}.

By comparison of the TG, DTG and Q-TG curves of the samples (Figs. 1 and 2) with the results of the lattice defects it follows that the formation of boehmite [reaction according to eqn. (1)] is suppressed by an increase in the lattice defects in the crystal and a decrease in the primary particle size. The most highly disturbed artificial hydrargillite (sample III) shows approximately the same decomposition behaviour as in the case of natural hydrargillite (sample IV). However, with sample III the decomposition according to eqn. (2) already begins at low temperatures as high-energy amorphous hydrargillite is formed to a large extent by the grinding process.

The effect of the lattice defects on the decomposition behaviour of the hydrargillite must be considered in relation with its lattice structure. Hydrargillite forms a double-layer structure of the brucite type [$Mg(OH)_2$] in which the octahedron vacancies in the double layers of the OH ions are occupied by cations [9,10]. As opposed to brucite, in the case of hydrargillite the sequence of layers of the OH ions is /AB/BA/AB/BA/, where the OH ions in the AB layers are deformed and have a smaller distance of 0.203 nm as against 0.236 nm with the hexagonal closest packing. Between the double layers the structure is somewhat dispersed (distance 0.281 nm). With artificial hydrargillite stacking of the packets of the layer is shifted to the *a*-axis so that the monoclinic structure is formed. With natural hydrargillite there is an additional shift to the *b*-axis resulting in the triclinic structure. Structure channels are formed in such a way that the aluminium ions occupy only two-thirds of the present octahedron vacancies.

From the structure of both artificial and natural hydrargillite it can be seen that there exist structurally favoured chances for the migration of OH ions or H_2O molecules. These are the dispersal between the double layers and the structure channels. This mechanism has already been discussed by Rouquerol et al. [11]. However, Sasvari and Zalai [12] give a model of the emission of whole OH layers. The obtained lattice defects (Table 1) of the hydrargillites amount to a maximum of approximately 10% of the distance of the OH double layers in the hydrargillite lattice. From this, an inhibition of the migration of OH ions and H_2O molecules through the lattice results.

The decomposition of such disturbed hydrargillite samples can only proceed with higher temperatures compared to the undisturbed material.

As could be seen from the thermodynamic considerations (see above), the formation of aluminium oxide [eqn. (2)] compared to that of boehmite [eqn. (1)] is favoured with increasing temperatures. Therefore, with increasing lattice defects only smaller boehmite components are formed during thermal decomposition and there is no boehmite formation at all with natural hydrargillite (sample IV) and ground artificial hydrargillite (sample III).

The fact that the emission of the OH ions or H_2O molecules between the packets of the OH double layers is complicated by the lattice defects and the suppression of the formation of boehmite is also based on the results of the thermal decomposition of the bayerite [β-$Al(OH)_3$]. According to Mackenzie [13] the decomposition of the bayerite was a single-stage process with formation of Al_2O_3. We have observed that the DTA peak temperature amounts to 290°C and the Q-TG step to 280°C under quasi-isothermal conditions in the labyrinth crucible, which is in the same temperature range as that of natural hydragillite (sample IV) corresponding to the reaction in eqn. (2). The absence of a boehmite formation is explained by the arrangement of the OH layers AB/AB/AB/AB as a closest packing without the expansions of the hydrargillite between the double layers.

Effect of the impurities

Hydrargillites always contain small amounts of sodium ions which are inserted into the lattice. Stimulated by the investigations of Asselmeyer [14] who found a decomposition temperature for europium-containing hydrargillite of approximately 100°C lower than that of the pure product, we performed a systematic investigation of artificial hydrargillites containing sodium, potassium and rubidium in the concentration range 0.04%–0.25% Me_2O (Me = Na, K and Rb, respectively). The DTA and Q-TG measurements showed no significant differences compared to the curves which we obtained on artificial hydrargillite containing Na_2O (curves 1 and 5, Fig. 1; curve 2, Fig. 2). Therefore we can say that alkali ions inserted into the hydrargillite lattice have no influence on the decomposition process even with increased ionic radius (Na < K < Rb).

Mechanism of the boehmite formation

Model conceptions as to the reaction mechanism of the decomposition of hydrargillite trace back to De Boer et al. [15,16]. According to this theory there exist hydrothermal conditions in the crystal, where inside the crystallites a water vapour overpressure is formed which causes the formation of boehmite. This theory appears to be understandable as the preparation of boehmite from hydrargillite with increased pressure proceeds quantitatively

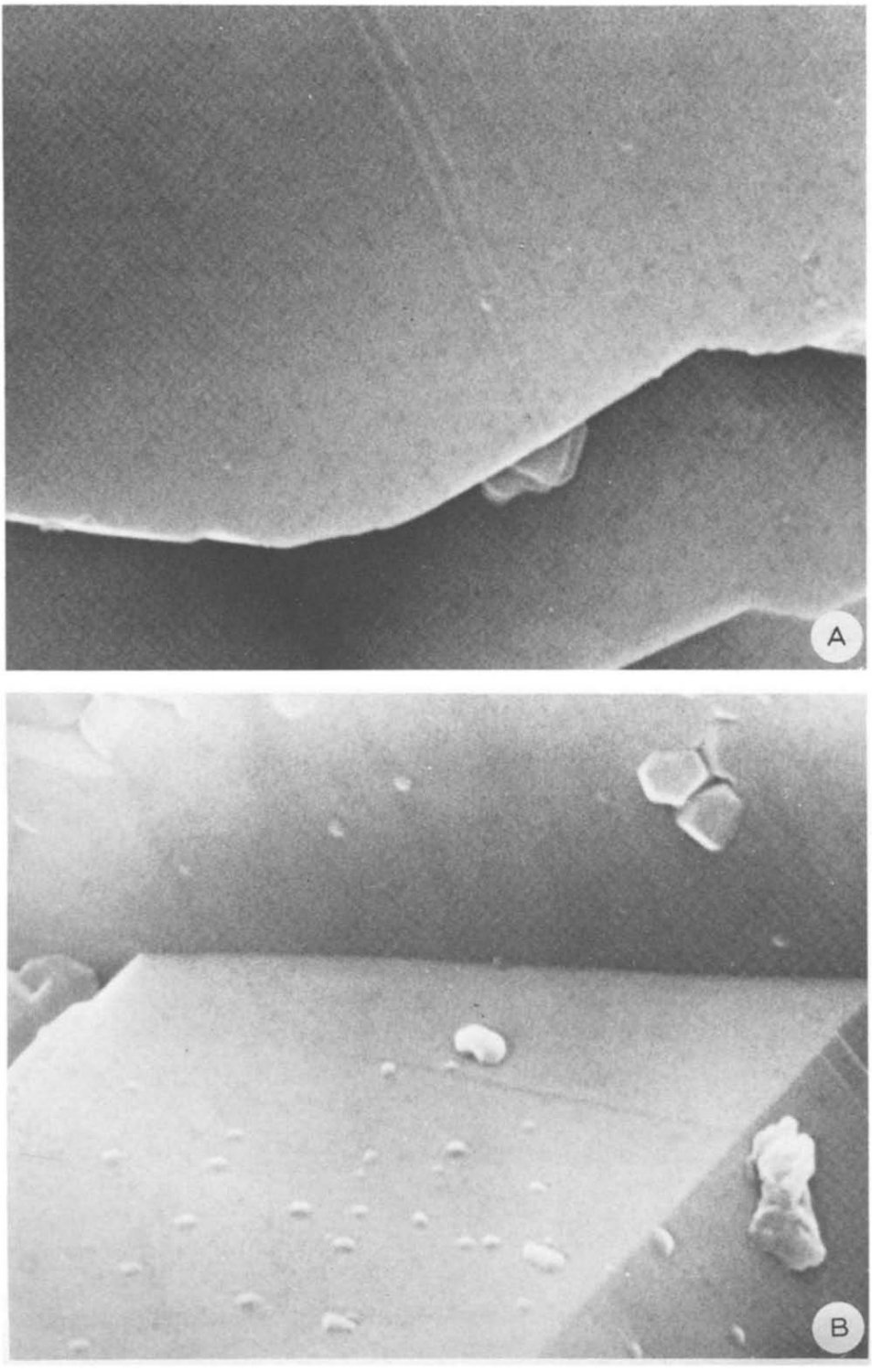

Fig. 5. Scanning electron micrographs of artificial hydrargillite (sample I); enlargement 1 : 22000 (image scale 22 mm ≙ 1μm). a, Initial material; b, thermally decomposed up to 4% weight loss in the derivatograph Q in a labyrinth crucible.

and, moreover, the formation of boehmite was observed with coarse material under thermoanalytical conditions [17]. In the literature different possibilities have been discussed concerning the formation of hydrothermal conditions. In most cases it was supposed that at the beginning of the reaction on the surface of the hydrargillite particles a layer of χ-Al_2O_3 is formed first which prevents leakage of water vapour from the inside of the crystals and favours the formation of boehmite. After rupture of this layer and leakage of the water vapour, formation of χ-Al_2O_3 goes on [13,18]. According to Lodding [19] the surface layer does not consist of χ-Al_2O_3, but of boehmite. The hydrothermal conditions must also be realized by the fact that the produced water vapour can only very slowly leave the pore system of the solid [16].

Our test results cannot be interpreted by means of the theories discussed in the literature. In the range of the boehmite formation a weight loss of hydrargillite up to approximately 10% can be observed (curve c, Fig. 4). This weight loss is in contrast to the formation of a gas tight film on the hydrargillite grains.

From the thermoanalytical results in Part I of this work [1] we concluded that a nucleation-controlled process is concerned with the formation of boehmite. The primary transformation centres can be visualized just as well in the phase-contrast microscope as in the scanning electron microscope.

Compared to the initial material, in addition to hydrargillite subcrystals, the scanning electron micrograph (Fig. 5) shows lenticular primary phases which are randomly distributed on the crystal surface. The size of these nuclei varies from 0.06 μm to 0.3 μm. Thus, the lower boundary corresponds to the primary particle size of the used hydrargillite with a size of 0.055 μm (Table 1, sample I). In the phase-contrast image these nuclei can be identified as a boehmite phase.

ACKNOWLEDGEMENTS

The authors wish to thank Prof. P. Brand and Prof. E. Pungor for valuable discussions, and also Dr. L. Wojnarovits, SZIKTI, Budapest, for the preparation of the scanning electron photographs.

REFERENCES

1 F. Paulik, J. Paulik, R. Naumann, K. Köhnke and D. Petzold, Thermochim. Acta, 64 (1983) 1.
2 J. Paulik and F. Paulik, in G. Svehla (Ed.), Analytical Chemistry, Vol. XII, Part A, Elsevier, Amsterdam, 1981.
3 F. Paulik and J. Paulik, J. Therm. Anal., 5 (1973) 253.
4 R. Fricke and E.C. Gwinner, Z. Phys. Chem., Abt. A, 183 (1938) 165.

5 A. Kochendörfer, Z. Kristallogr., 105 (1944) 393.
6 J. Barin, O. Knacke and O. Kubaschewski, Thermochemical Properties of Inorganic Substances, Springer-Verlag, Heidelberg, New York, 1977.
7 T.A. Korneva, T.S. Yusupov, L.G. Lukjanova and G.M. Gusev, Proc. Fourth Int. Conf. Therm. Anal., 1974, Vol. 2, Akadémiai Kiado, Budapest, 1975, p. 659.
8 L.G. Lukjanova, N.M. Lemina, T.A. Korneva, E.N. Zhukova and G.M. Gusev, Vsb. Fiz.-Khim. Issled. Mekhanicheski Aktivir. Mineraln. Veshchestr., (1975) 63.
9 H.D. Megaw, Z. Kristallogr., 87 (1934) 185.
10 H. Saalfeld, Neues Jahrb. Mineral., Abh., 95 (1960) 1.
11 J. Rouquerol, F. Rouquerol and M. Ganteaume, J. Catal., 36 (1975) 99.
12 K. Sasvari and A. Zalai, Acta Geol. Acad. Sci. Hung., 4 (1957) 415.
13 R.C. Mackenzie, Differential Thermal Analysis, Academic Press, London, New York, 1970, p. 283.
14 F. Asselmeyer, Z. Angew. Phys., 1 (1947) 26.
15 H.J. De Boer, J.M.H. Fortuin and J.J. Steggerda, Proc. K. Ned. Akad. Wet. B, 57 (1954) 170, 434.
16 H.J. De Boer, Angew. Chem., 70 (13) (1958) 383.
17 K. Wefers and G.M. Bell, ALCOA (Alum. Co. Am.) Res. Lab., Tech. Pap. No. 19 (1972) 8, 36.
18 P. Chatelain and Ch. Maughin, C.R. Acad. Sci., 241 (1955) 46.
19 W. Lodding, Proc. Int. Conf. Therm. Anal., 1968, Vol. 2, Academic Press, New York, 1969, p. 1239.